environmental microbiology

Environmental Microbiology (2019) **21**(1), 152–163 doi:10.1111/1462-2920.14435

Iron- and aluminium-induced depletion of molybdenum in acidic environments impedes the nitrogen cycle

Xiaoxuan Ge,[1†] Brian J. Vaccaro,[1†] Michael P. Thorgersen,[1] Farris L. Poole II,[1] Erica L. Majumder,[2] Grant M. Zane,[2] Kara B. De León,[2] W. Andrew Lancaster,[1] Ji Won Moon,[3] Charles J. Paradis,[4] Frederick von Netzer,[5] David A. Stahl,[5] Paul D. Adams,[6] Adam P. Arkin,[6] Judy D. Wall,[2] Terry C. Hazen[4] and Michael W. W. Adams [1*]

[1]*Department of Biochemistry and Molecular Biology, University of Georgia, Athens, GA, 30602, USA.*

[2]*Department of Biochemistry, University of Missouri, Columbia, MO, 65211, USA.*

[3]*Environmental Sciences Division, Oak Ridge National Laboratory, Oak Ridge, TN, 37830, USA.*

[4]*Department of Civil and Environmental Engineering, University of Tennessee, Knoxville, TN, 37996, USA.*

[5]*Department of Civil and Environmental Engineering, University of Washington, Seattle, WA, 98495, USA.*

[6]*Lawrence Berkeley National Laboratory, Berkeley, CA, 94720, USA.*

Summary

Anthropogenic nitrate contamination is a serious problem in many natural environments. Nitrate removal by microbial action is dependent on the metal molybdenum (Mo), which is required by nitrate reductase for denitrification and dissimilatory nitrate reduction to ammonium. The soluble form of Mo, molybdate (MoO_4^{2-}), is incorporated into and adsorbed by iron (Fe) and aluminium (Al) (oxy) hydroxide minerals. Herein we used Oak Ridge Reservation (ORR) as a model nitrate-contaminated acidic environment to investigate whether the formation of Fe- and Al-precipitates could impede microbial nitrate removal by depleting Mo. We demonstrate that Fe and Al mineral formation that occurs as the pH of acidic synthetic groundwater is increased, decreases soluble Mo to low picomolar concentrations, a process proposed to mimic environmental diffusion of acidic contaminated groundwater. Analysis of ORR sediments revealed recalcitrant Mo in the contaminated core that co-occurred with Fe and Al, consistent with Mo scavenging by Fe/Al precipitates. Nitrate removal by ORR isolate *Pseudomonas fluorescens* N2A2 is virtually abolished by Fe/Al precipitate-induced Mo depletion. The depletion of naturally occurring Mo in nitrate- and Fe/Al-contaminated acidic environments like ORR or acid mine drainage sites has the potential to impede microbial-based nitrate reduction thereby extending the duration of nitrate in the environment.

Received 24 July, 2018; revised 24 September, 2018; accepted 27 September, 2018. *For correspondence. E-mail adamsm@uga.edu; Tel. +706-542-2060; Fax +706-542-0229. †These authors contributed equally to this work.

Introduction

Nitrate contamination has become a serious environmental issue due to the extensive use of nitrate-containing fertilizers in agriculture as well as through the release of nitrate-containing industrial wastes (Bouchard *et al*., 1992). The natural nitrate concentration in groundwater is typically less than 2 mg/l (Nolan *et al*., 1998) and the U.S. Environmental Protection Agency's (EPA) maximum contaminant level (MCL) for nitrate (as the nitrate ion) in drinking water is 50 mg/l (0.80 mM). High nitrate concentrations can be detrimental to health and is known to cause methemoglobinemia in infants and adults (Powlson *et al*., 2008; Gorchev and Ozolins, 1984). In 2006, 1.9 million people in the United States were predicted to use drinking water from private wells with ≥ 5 mg/l (0.08 mM) nitrate (Nolan and Hitt, 2006). Additionally, nitrate persistence in rivers can increase nitrate eutrophication near major river outlets resulting in algal blooms, hypoxia, and dead zones (Diaz and Rosenberg, 2008; Gruber and Galloway, 2008).

Mo is a key element in the global nitrogen cycle (Fig. 1A). It is the catalyst in three enzyme-based processes, N_2-fixation (nitrogenase), nitrification (nitrite oxidoreductase), denitrification (nitrate reductase) and dissimilatory nitrate reduction to ammonium (DNRA; nitrate reductase) (Zhang and Gladyshev, 2008). In fact, low environmental and/or dietary Mo appears to promote oral (Khanna *et al*., 2013), esophageal (Jackson *et al*., 1986; Nouri *et al*., 2008) and gastric (Cao *et al*., 1998) cancers in humans due to decreased reduction of nitrate and nitrosamine. In natural environments, the concentration of Mo can limit the efficiency of key Mo-dependent

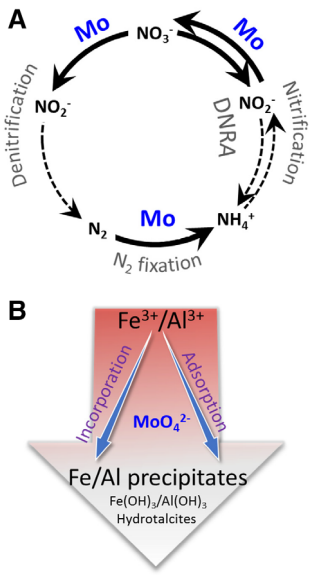

Fig. 1. Mo in the nitrogen cycle and at ORR. A. Mo-dependent steps in the nitrogen cycle are indicated by bold black arrows while dashed arrows are independent of Mo (dissimilatory nitrate reduction to ammonium [DNRA]). B. Model of Mo depletion at the ORR contaminated site. The large background arrow indicates pH change of contaminated groundwater from lower pH (red) to higher pH (pink to white). Two mechanisms of Mo depletion by Fe and/or Al precipitates are proposed: incorporation and adsorption as indicated by blue arrows. [Color figure can be viewed at wileyonlinelibrary.com]

reactions (Barron *et al*., 2009; Glass *et al*., 2012). Thus, natural or anthropogenic processes that deplete aquatic environments of Mo may have profound effects on the rate of steps in the global nitrogen cycle (Zhang and Gladyshev, 2008).

The major soluble form of Mo in natural environments is as the oxyanion molybdate (MoO_4^{2-}) (Moura *et al*., 2004). However, there are several ways in which soluble molybdate can be removed from the environment, including by binding to existing insoluble minerals or by being incorporated into insoluble minerals as they are formed. For example, molybdate is precipitated from sea water in the form of molybdenum-iron–sulfur compounds present in black shales and sea sediments (Helz *et al*., 1996). Molybdate is also known to bind to insoluble organic matter in top soils (Wichard *et al*., 2008). In addition, molybdate can be incorporated into hydrotalcite minerals that are formed by the precipitation of iron (Fe) and aluminium (Al) oxy/hydroxides (Allada *et al*., 2002; Smith *et al*., 2005; Paikaray and Hendry, 2013). Molybdate can also adsorb directly to insoluble minerals such as ferrihydrite ($Fe_2O_3 \cdot xH_2O$) and gibbsite ($Al(OH)_3$) (Gustafsson, 2003; Goldberg, 2010). This Mo depletion process caused by iron or aluminium minerals is pH-dependent where molybdate concentration decreases as the pH increases from pH 3.1 to 6.3 for Fe precipitates, or from pH 5.5 to 6.7 for Al precipitates (Allada *et al*., 2002; Gustafsson, 2003; Smith *et al*., 2005; Goldberg, 2010; Paikaray and Hendry, 2013). However, it is not clear if these mechanisms are effective at depleting molybdate from solution in a regime that limits Mo bioavailability in natural environments (Thorgersen *et al*., 2015).

At Oak Ridge Reservation (ORR) in Tennessee, USA between 1951 and 1983, the U.S. government disposed of millions of litres of waste containing nitric acid and toxic metals. The waste generated from uranium operations at the Y-12 Plant was discarded into four unlined earthen reservoirs referred to as the S-3 ponds (~ 9.5 million litres per pond) (Brooks, 2001). In 1978, the pH values of the ponds ranged from 0.8 to 5.3 and contained nitrate at concentrations up to 1.2 M (Brooks, 2001). Metals present included iron up to 21 mM, aluminium up to 178 mM and uranium up to 1.3 mM (Brooks, 2001). In 1983, in an effort to clean-up the waste site, the pH in the S-3 ponds was adjusted to about 9 (Brooks, 2001; Revil *et al*., 2013). The sludge that formed was allowed to settle and the liquid waste was removed (Brooks, 2001). In 1988 the 1-m-thick sludge was stabilized with coarse aggregates and the S-3 ponds were filled and capped with a parking lot (Revil *et al*., 2013). In 1997, an analysis of the groundwater in 46 wells surrounding the parking lot revealed that there was a plume of nitrate that extended approximately 1 km to a depth of over 100 m (Kornegay *et al*., 1994; Jones, 1998). In the most recent survey at ORR in 2015, groundwater from wells in the contamination plume were still at low pH range (pH 3–5) and contained high concentrations of nitrate (up to 230 mM) and various metals, including uranium (up to 0.6 mM) (Smith *et al*., 2015; Thorgersen *et al*., 2015). Interestingly, of 26 metals analyzed, molybdenum (Mo) was the only metal that had a lower median concentration (<< 1 nM) in the highly contaminated wells compared with pristine wells (up to 330 nM) (Thorgersen *et al*., 2015). In essence, the highly contaminated wells were depleted in Mo and the reason for Mo depletion and its possible biological effects are the focus of the present study.

In the ORR contaminated environment many factors could limit microbial activity including low pH, fluctuations in dissolved oxygen and the availability of reduced carbon (Rauret, 1998; Istok *et al*., 2004; Giles *et al*., 2012). We previously proposed that low concentrations of Mo observed in the contaminated environment could limit microbial nitrate reduction (Thorgersen *et al*., 2015). Herein we seek to examine the cause of Mo-depletion in the contaminated environment. We propose an environmental model in which molybdate depletion is a result of adsorption and/or incorporation of Mo into Fe and Al minerals that form as the pH of contaminated acidic groundwater increases through mixing with the surrounding neutral groundwater and sediment (Fig. 1B). Evidence supporting the Fe- and Al-dependent Mo-depletion model is provided including synthetic groundwater studies and metal analysis of vertical soil cores drilled in an ORR non-

contaminated site and a contaminated area near the S-3 ponds. Importantly, we demonstrate that Fe- and Al-induced Mo-depletion results in a Mo concentration regime that limits microbial nitrate reduction by the ORR groundwater isolate *Pseudomonas fluorescens* strain N2A2.

Results

Concentrations of nitrate, Mo, Al and Fe in ORR groundwater

In a previous study, groundwater samples from 93 ORR wells were analyzed for multiple geochemical parameters (Smith *et al*., 2015). The concentrations of nitrate, Al, Fe and Mo, as well as the pH of those groundwater samples are re-analyzed and plotted in Fig. 2. There is a subset of groundwater samples from wells located near the S-3 ponds that are highly contaminated with nitrate (> 1 mM) and are very acidic (pH < 4). These samples have much lower Mo concentrations (<< 1 nM) compared with samples from pristine wells, located over 3 km from the S-3 ponds, (pH > 6 and nitrate concentration < 0.80 mM), where Mo concentrations reach up to 300 nM (Fig. 2A and Supporting Information Fig. S1). The groundwater samples from these highly contaminated wells have Fe concentrations less than 3 μM while Al concentrations are as high as 20 mM (Fig. 2B and C).

Abiotic depletion of trace MoO_4^{2-} with Fe^{3+} or Al^{3+} precipitation

To test our Mo depletion model in the laboratory, Fe or Al treatment experiments were carried out with synthetic groundwater to determine if we could simulate Mo removal by Fe^{3+} and Al^{3+} precipitation. Specifically, the synthetic groundwater contained oxyanions that might compete with molybdate (3.1 mM HCO_3^- and 15.2 mM SO_4^{2-}), together with cations (8.9 mM Mg^{2+}) known to promote the formation of Fe- and Al-based minerals (hydrotalcites). These oxyanions and cations were added at concentrations mimicking what was measured in highly contaminated groundwater samples from wells near the S-3 ponds (Smith *et al*., 2015). Both the Fe and Fe + Al treatments were extremely efficient in depleting the synthetic groundwater of molybdate. As shown in Fig. 3A, the Fe $(NO_3)_3$ (20 mM) introduced a high concentration of contaminating Mo (47 nM) to the synthetic groundwater. When the pH was adjusted from 2.3 to 4.0, almost all Fe was removed from the solution, with only about 12 μM of the 20 mM remaining after Fe treatment and about 13 μM after Fe + Al treatment. At the same time, the Mo was depleted to below the detection limit (< 5 pM) of the ICP-MS instrument after both Fe and Fe + Al treatments. When the pH was increased to 6.7, only 0.28 and 0.47 μM Fe remained in solution after Fe and Fe + Al treatments respectively. Correspondingly, the Mo concentrations measured were 170 and 556 pM. We determined that the additional Mo was introduced as a contaminant from the trace grade NaOH that was used to adjust the pH (Fig. 3A, left panel). It should be noted that the solubility of molybdate is independent of pH over this range (pH 4.0–6.7) and is unaffected by the pH adjustment in the control solutions (without added Fe, Fig. 3B).

Al was not as efficient as Fe or Fe + Al at removing low concentrations of Mo from synthetic groundwater at pH 4.0 or at 6.7. Addition of Al (as the nitrate salt) introduced only 3.5 nM Mo as a contaminant. When the pH was increased to 4.0 after Al addition (from pH 3.8), only a small fraction of the Al precipitated changing the concentration from 19.7

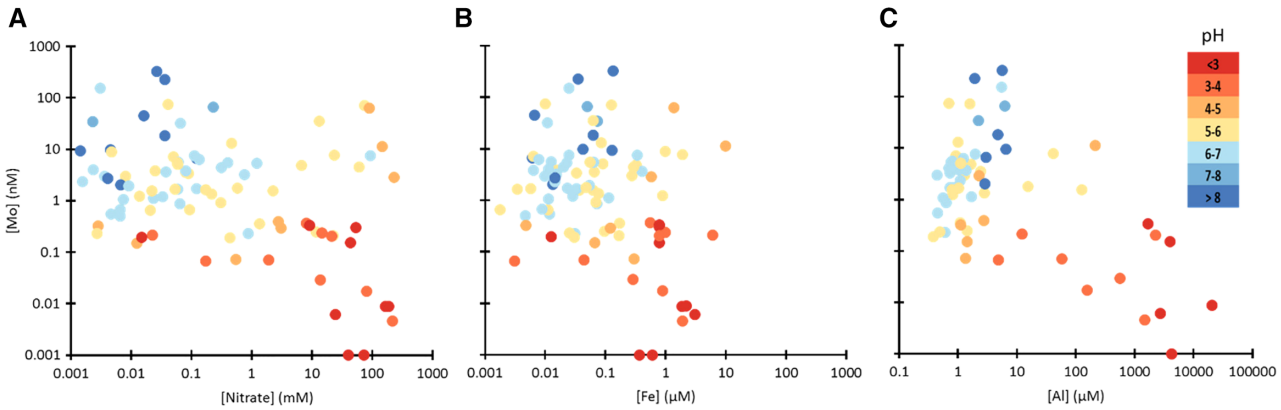

Fig. 2. Nitrate, Fe, Al and Mo concentrations in ORR groundwater samples at various pH levels. A. Nitrate and Mo concentrations in groundwater samples from different ORR wells. Each data point represents a groundwater sample from a well. A total of 93 samples were taken from 80 wells. Different colours represent the pH of each well from low (in red) to high (in blue). The X axis indicates the nitrate concentration of each sample in mM, while the Y axis indicates the Mo concentration detected of each sample in nM. The concentrations are plotted on logarithmic scales. Similar plots are drawn to show the relationship between Fe and Mo concentrations (B) as well as Al and Mo concentrations (C) in groundwater from different ORR wells. All samples were measured in duplicate and average values are reported. Wells that are pH > 6 and have nitrate concentrations < 0.80 mM are considered pristine wells. [Color figure can be viewed at wileyonlinelibrary.com]

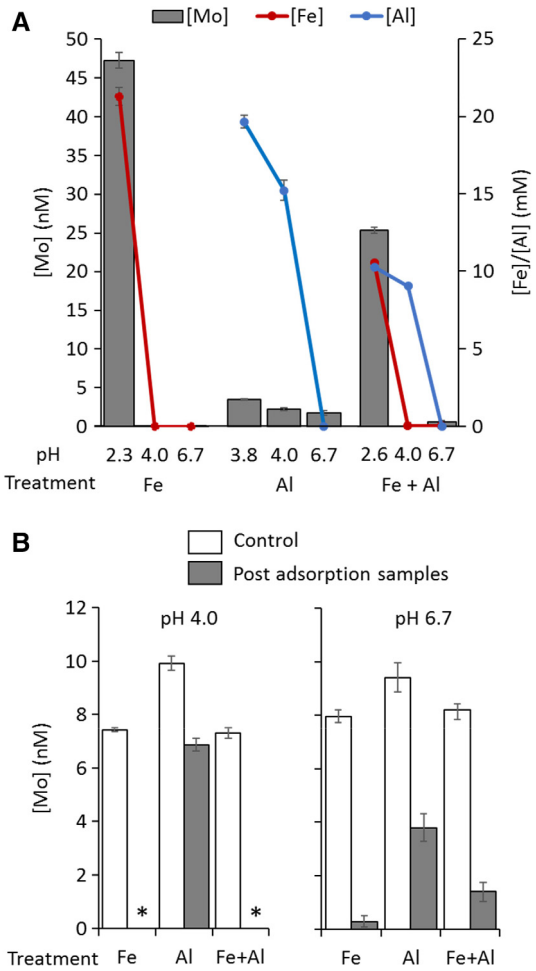

Fig. 3. Mo depletion in synthetic groundwater. A. Mo depletion in synthetic groundwater induced by Fe, Al or a combination of Fe and Al precipitation at pH 4.0 and pH 6.7. Mo concentrations of three groups of samples at different pH are indicated by grey bars. The first bars indicate Mo concentrations in synthetic groundwater before pH adjustment with the following bars indicating Mo concentrations after pH adjustment and the pH for each sample is indicated below each bar. The concentrations of free Fe (red lines) and free Al (blue lines) are also indicated in this figure in mM. B. Mo adsorption to Fe-, Al- or a Fe + Al-precipitates at pH 4.0 (left) and pH 6.7 (right). Samples were first Mo depleted by the given treatment and pH to generate precipitates. Then half of the supernatant for each sample was removed for the control (white bar), and the remaining supernatant and precipitate was used as the sample (black bar). Additional Mo was added to the control and sample, incubated overnight and then the soluble Mo was measured. *Mo concentrations below the detection limit of ICP-MS. [Color figure can be viewed at wileyonlinelibrary.com]

to 15.3 mM. Accordingly, the Mo concentration decreased from 3.5 to 2.2 nM. Increasing the pH to 6.7 dramatically increased Al precipitation with only 6.1 μM remaining in solution (from 15.3 mM), but the Mo concentration only decreased to 1.7 nM (from 2.2 nM; we estimate that 10% of this difference was introduced as a contaminant from the NaOH) (Fig. 3A, middle panel). As shown in Fig. 3A, when both Al and Fe were present in synthetic groundwater, the results appeared to be additive and there were no dramatic synergistic effects caused by both metals precipitating from the same solution, especially at pH 4.0, only about 1.0 mM Al precipitated out of 10.3 mM present in the synthetic groundwater.

Several anions, including NO_3^-, HCO_3^-, SO_4^{2-} and Cl^-, are present in the ORR groundwater (Smith *et al*., 2015) and were added to the synthetic groundwater in the experiments above. In this case, the synthetic groundwater contained one of the following ions: sulfate (15.2 mM), bicarbonate (3.0 mM), phosphate (5.0 mM) or chloride (10.5 mM) or a combination of sulfate (15.2 mM), bicarbonate (3.0 mM) and chloride (10.5 mM) (Supporting Information Table S1). As shown in Supporting Information Fig. S2A, depletion of Mo by Fe treatment was more or less independent of the presence of the anions, as all Mo concentrations decreased from approximately 50 nM to less than 400 pM. However, sulfate inhibited molybdate depletion in Al treatment as the Mo concentration was 2.2 nM (sulfate only) and 3.4 nM (combination of sulfate, carbonate and chloride, SCC). Hence, sulfate interferes with Mo removal by Al precipitation, but not Fe precipitation which explains why nM levels of Mo remained in Al-treated synthetic groundwater even at pH 6.7 (Fig. 3A).

We next addressed the question of whether molybdate could also be adsorbed by pre-formed Fe or Al precipitates from synthetic groundwater. As shown in Fig. 3B, at pH 4.0 the pre-formed Fe-precipitates scavenged Mo from solution and decreased soluble Mo from 10 nM to 200 pM. At pH 6.7 the Mo concentration decreased further to less than 5 pM (below the detection limit). The pre-formed Al-precipitates were less effective in removing Mo, decreasing the concentration to 6.9 nM at pH 4.0 and to 3.7 nM at pH 6.7. Importantly, the pre-formed Al precipitate did not impede Mo uptake by the pre-formed Fe-precipitate at pH 4.0 but they did prevent Mo adsorption by the pre-formed Fe-precipitate at pH 6.7, resulting in a concentration of remaining Mo fivefold higher (2.0 nM) in samples with both Fe and Al precipitates (Fig. 3B). Fe precipitation in synthetic groundwater at low pH is more efficient than Al precipitation, which is consistent with the observation that no significantly high concentrations of Fe (> 10 μM) were detected in any of the contaminated wells while much higher concentrations of Al were measured (up to ~ 20 mM; Fig. 2). The data presented here therefore suggest that Mo depletion in ORR groundwater is predominantly a result of both incorporation and adsorption to Fe-based oxyhydroxides precipitates, but that Al-based precipitates could also play a role.

Co-occurrence of recalcitrant Mo with Fe and Al in contaminated ORR sediment

In order to analyze Mo concentrations and its bioavailability in ORR sediment, a sediment core adjacent to the S-3

ponds contamination source (EB-106) and a sediment core not contaminated by the S-3 plume (EB-271) were obtained. The cores were divided into 23 cm segments by depth (800 and 450 cm total), which were extracted and analyzed for metals using the modified BCR three step sequential extraction procedure (Rauret, 1998) that involves a series of increasingly harsh treatments to release metals from the sediment. As shown in Supporting Information Fig. S3A,C, Mo was not detected in the weak acid extracted fractions (pH 3.0) of the first extraction step or in the reducible extraction fractions for either core. Low amounts of Mo (< 2 mg/kg and < 0.7 mg/kg, respectively) were released in this final and much harsher extraction step of the contaminated and non-contaminated cores. There was some Mo in the vadose zone of both wells (100 cm depth and 194 cm depth) of the cores that may have been associated with organic matter. There were also three Mo concentration maxima centred at 501, 583 and 674 cm depth in the saturated zone of the contaminated core (Supporting Information Fig. S3A,B) and a feature of Mo extending into the saturated zone of the non-contaminated core from 331 to 444 cm depth (Supporting Information Fig. S3C,D).

Total metals were also measured for both sediment core segments using a separate microwave digestion procedure by nitric acid (Supporting Information Fig. S3A,C). Importantly, for the non-contaminated core, similar amounts of Mo were measured by the two different procedures (Supporting Information Fig. S3C). Conversely, for the contaminated core, approximately 60% more Mo was measured in the vadose zone and approximately two- to threefold increased Mo was measured in the three saturated zone maxima by the total digestion method compared with the oxidizing step of the sequential extraction procedure (Supporting Information Fig. S3A). This result suggests that there is a population of highly recalcitrant Mo in the contaminated core that is only observable with total digestion of the sediment in nitric acid that is not present in the non-contaminated core.

The concentrations of Fe and Al found in the contaminated ORR sediments by the total extraction method are shown in Supporting Information Fig. S3B, along with those for Mo. The Fe data show that there is one major maximum and several minor ones, and while the Al data show more variation between the triplicate environmental samples, there are clearly several major concentration maxima. Interestingly, of the three major Mo maxima in the saturated zone, two of them (501 and 583 cm) correspond to major (501 cm) and minor (583 cm) maxima for both Fe and Al. The major Mo concentration maximum at 674 cm does not appear to correlate with either of the other metals. For the non-contaminated core no significant maxima of Mo correspond to those of Fe or Al (Supporting Information Fig. S3D).

Nitrate removal limited by Mo depletion

To test the impact of Fe- and Al-dependent Mo depletion on microbial action (Fig. 1A), the nitrate removal activity of a denitrifying microorganism isolated from ORR groundwater, *Pseudomonas fluorescens* N2A2, was investigated after its growth medium was depleted of Mo by Fe- or Al-based precipitation (Supporting Information Table S1). The measured Mo concentrations in the growth media decreased from 32.7 nM to 400 pM as a result of Fe treatment and from 13.7 nM to 800 pM as a result of Al treatment (Supporting Information Table S2). Strain N2A2 grew very poorly in both of these Mo-depleted media compared with the standard medium containing 10 nM Mo (Fig. 4A). However, growth was almost fully restored upon the subsequent addition of 10 nM MoO_4^{2-}, showing that the Fe- and Al-induced precipitation did indeed inhibit growth by removing soluble Mo (Fig. 4A). However, Mo addition did not restore growth completely (Fig. 4A), so it is possible that the Fe- and Al-treatments decreased the concentration of one or more of the other medium components required for optimal growth of strain N2A2 (Fig. 4A).

While removal of soluble Mo by Fe- or Al-induced precipitation clearly impacts microbial growth, a more fundamental question is whether these processes also lead to a decrease in the ability of the ORR microorganism to catalyze nitrate removal with nitrate reductase, a Mo dependent enzyme that also contains Fe (Zumft, 1997). As shown in Fig. 4B,C, this conjecture proved to be the case. N2A2 cells in the Fe-treated medium (containing 400 pM Mo) removed only 16% of the nitrate that was initially present (60 mM), while more than 95% of the nitrate was removed by cells in the untreated medium (containing 10 nM Mo). About 40% of the nitrate was removed by cells in the Al-treated medium (containing 800 pM Mo). When Mo was added back to both the Fe- and Al-treated media, more than 80% of the nitrate was removed showing that Mo depletion was the cause of the nitrate removal deficiency in Fe and Al treated media (Fig. 4B).

Molybdenum is part of the catalytic site of nitrate reductase and the catalytic activity of the enzyme is directly related to its Mo content (Vergnes *et al*., 2004; Schwarz *et al*., 2009). Consequently, one would expect the amount of nitrate removed by N2A2 in a given environment to be directly related to the catalytic activity of its nitrate reductase and hence its Mo content. As shown in Fig. 4C, this expectation was the case. The total catalytic activity (units/mg of total cellular protein) of nitrate reductase was initially proportional (in early log phase, 28 h) to the Mo concentration in the medium. That is, cells had up to four-fold higher nitrate reductase activity in media that had not been Mo depleted, or that had been supplemented with Mo after Fe- or Al- treatment (Fig. 4C). For

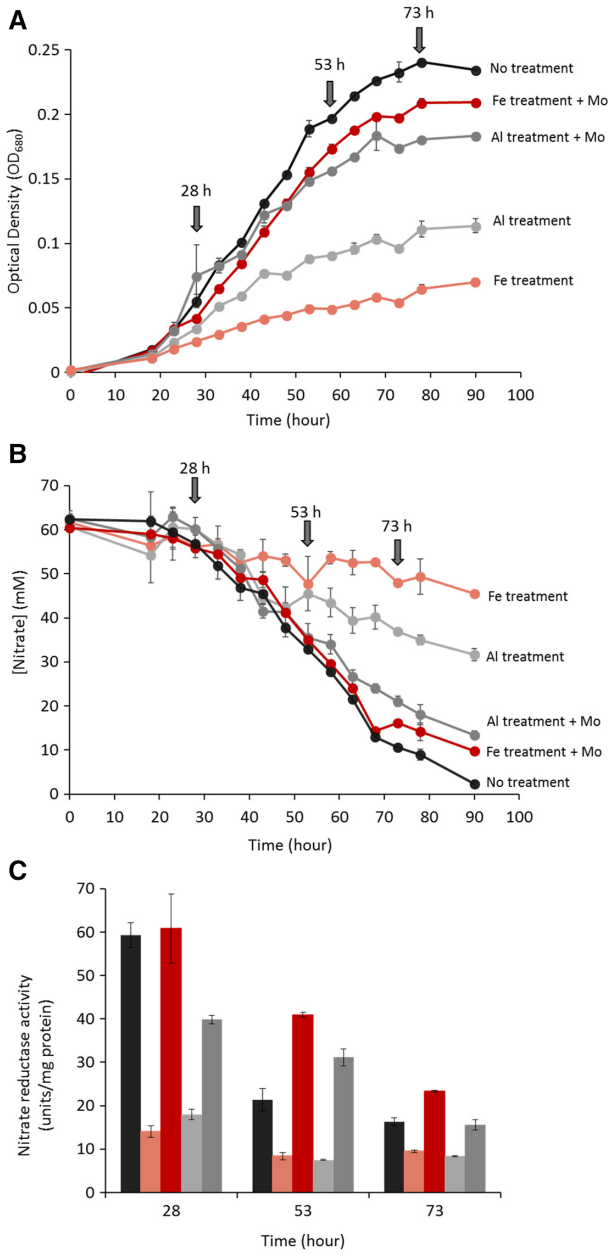

Fig. 4. Growth and nitrate consumption of ORR isolate N2A2 in Mo depleted and replete media. A. Growth curves of N2A2 in no treatment media (black line), Mo depleted media resulting from Fe treatment (pink line) or Al treatment (light grey line), and in Mo replete media after Fe treatment (red line) or Al treatment (dark grey line). Mo concentrations in different cultures were measured by ICP-MS and indicated in Supporting Information Table S2. B. Nitrate remaining during the growth of N2A2 in Mo depleted and replete media. C. Nitrate reductase activity of N2A2 at early log phase (28 h), middle log phase (53 h) and early stationary phase (73 h) under various growth conditions. The total nitrate reductase activity is expressed as units/mg, where 1 unit equals to 1 μmol nitrate reduced/min. The colours of different samples in (B) and (C) are consistent with those in (A). Arrows indicate the time points for enzyme activity assays. [Color figure can be viewed at wileyonlinelibrary.com]

example, the highest nitrate reductase activity is about 60 units/mg in Fe-treated media with Mo supplementation while only about 15 units/mg activity was detected in Fe-treated media at 28 h. However, the cellular production of the nitrate reductase protein is dependent upon the nitrate-content of the medium (Showe and DeMoss, 1968; Härtig *et al*., 1999) so in Mo-sufficient media the specific activity of the enzyme decreases as the nitrate is removed (at middle log phase, 53 h, and early stationary phase, 73 h, Fig. 4C). In contrast, in the Fe- and Al-depleted media, the specific activities of the enzyme do not change dramatically and remain low over time. Hence, with abundant Mo, the specific activity of the nitrate reductase reflects the amount of nitrate reductase protein that is produced. In contrast, in Fe- and Al-treated media, the measured nitrate reductase activity reflects the prevailing Mo-depletion conditions, independent of the nitrate concentration or the amount of nitrate reductase protein. Mo is therefore the key to catalytic activity and thus to efficiency in the nitrate removal process.

Discussion

This study combines Mo depletion in acidic and metal contaminated ORR groundwater and nitrate reduction by microorganisms into one environmental model. The liquid in the S-3 ponds was highly acidic (pH < 0.8) as a result of the high concentrations of contaminating nitric acid present. The results presented herein show that Fe^{3+} and Al^{3+} are effective at removing molybdate from solution, even at the extremely low (< 10 nM) starting concentrations found in the ORR environment. Mo removal at ORR appears to occur as a result of either adsorption onto pre-formed Fe- and Al-based oxy/hydroxides or by incorporation into Fe- and Al-based minerals that form as the pH of the acidic groundwater gradually increases (to pH > 3) as it flows into the surrounding sediment (Brooks, 2001; Revil *et al*., 2013; Smith *et al*., 2015).

The sediment at ORR is rich in Fe-oxides (Watson *et al*., 2004; Wu *et al*., 2006) and acidic dissolution of magnetite occurs in nitric acid at pH < 2.0 (Salmimies *et al*., 2011; Salmimies, 2012). This Fe^{3+} in turn would precipitate when the pH increases as a result of dilution with fresh groundwater or by interactions with carbonated soils thereby scavenging soluble Mo (Revil *et al*., 2013). We show here that Fe^{3+} is extremely effective at removing soluble Mo from synthetic groundwater at pH values as low as 4.0, while a pH closer to neutral is required for Al^{3+} to scavenge Mo. That iron rather than aluminium is the primary driver of Mo depletion in the ORR environment is consistent with our elemental analyses of the contaminated ORR wells (pH < 5.0), in which the Fe concentrations are extremely low (μM range) but Al persists (mM range) and Mo is virtually undetectable. We contend that Fe precipitation at low pH has already removed Mo from the groundwater of the highly contaminated wells near the S-3 ponds. In addition, the measurement of a

recalcitrant population of Mo that could only be observed when sediment was completely digested in nitric acid that was present in the contaminated but not the non-contaminated core supports our environmental model. That several of the Mo concentration maxima (at 501 and 583 cm depth) observed in the contaminated core coincides with Fe and Al maxima also supports the model.

We show here that pH-induced precipitation of Fe-oxy/hydroxides, and to a lesser extent those that are Al-based, cause depletion of soluble Mo resulting in Mo concentrations in the low pM range and in many cases beyond the detection limit (< 5 pM). While such low Mo concentrations are consistent with those measured in the highly contaminated groundwater at ORR, they are also at the limits of experimental design, particularly when attempting to grow microorganisms in the laboratory. Mo is a contaminant in virtually all chemicals used in microbial growth media, especially in SO_4^{2-}, PO_4^{3-}, Fe^{3+} and HCO_3^-, which are added to Mo-depleted media. Even though we used trace grade chemicals, Mo was still introduced to the media as a contaminant at concentrations greater than 100 pM. In other words, it was nearly impossible to reproduce the extent of Mo limitation in the highly contaminated ORR groundwater in the laboratory because of unavoidable Mo contamination in commercial chemicals.

Thus, the lowest Mo concentrations we could prepare experimentally for growth experiments involving the ORR-denitrifying strain *Pseudomonas fluorescens* N2A2 were in the 100 pM range, which was sufficient to demonstrate a negative impact on nitrate reduction. Yet, the Mo concentration in highly contaminated ORR groundwater is less than 10 pM, which is at least one order of magnitude lower than what we can simulate in the laboratory. Mo availability consequently has the potential to be a major limitation for the removal of nitrate by microorganisms in the ORR environment. Other potential barriers to nitrate reduction in the contaminated ORR environment include sources of reductant for denitrification (either organic or inorganic), the acidic conditions and the effects of heavy metal contaminants. Oxygen in sediments and groundwater can also affect denitrification, because oxygen is known to inhibit the transcription or the metabolic activity of related enzymes in most denitrifying microorganisms (Zumft, 1997; Qu *et al*., 2016). Natural microbiota can affect major geochemical cycles like the nitrogen cycle (Klotz and Stein, 2008; Hug *et al*., 2016), however inadequate metagenomic studies on sediment microbial communities in the ORR contaminated area leave unanswered questions about the relationships between these microbial communities and the environment. While denitrifiers or denitrifying communities that can survive at low pH or in the presence of certain heavy metal contaminants have been studied (Watanabe *et al*., 2001; Hemme *et al*., 2010; Palmer *et al*., 2010, 2012), conditions at the ORR site are extreme because of the complex contamination of multiple heavy metals combined with high concentrations of anions like nitrate, sulfate and chloride, as well as low pH (3–5). From the results presented herein, we contend that Mo limitation is another factor that could be impacting microbial nitrate reduction at ORR. Isolation of a nitrate-reducing microorganism able to grow in the presence of the high concentrations of a range of heavy metals found in some of the ORR wells, such as FW-126 (Smith *et al*., 2015), that is also able to utilize Mo at low pM or even fM concentrations would be of great interest.

Natural Mo concentrations in groundwater are rarely seen in the pM range like they are in the ORR contaminated groundwater. Typically Mo concentrations range from several nM to hundreds of nM (Smedley and Kinniburgh, 2017). However, low Mo concentrations have been observed, such as in the Wadden Sea and Boston Harbour (< 20 nM) and the Yorkshire Chalk aquifer (< 10 nM). The low Mo concentrations at these sites were proposed to be the result of Fe sedimentary mineralization and/or Mn oxide immobilization under sulfate-reducing conditions (Smedley and Edmunds, 2002; Morford *et al*., 2007; Beck *et al*., 2008). Low Mo concentrations (< 5–70 nM) resulting from the lower solubility of molybdate at low pH have also been reported in naturally acidic groundwater (pH 2.4–2.9) (Nordstrom, 2015). While the ORR environment can be considered unique, acid mine drainage (AMD) forms a similar highly acidic, metal-rich environment, which is generated from the drainage of pyrite oxidation and results in sulfuric acid and ferric iron contamination (Sánchez-España *et al*., 2016). Like the ORR plume, AMD is neutralized by mixing and dilution with nearby soils and groundwater. AMD can also dissolve aluminium, iron and other metals from various minerals and in general has high concentrations of Fe^{3+} and/or Al^{3+} (Cronan and Schofield, 1979; Sánchez-España *et al*., 2016).

To date, most remediation studies of AMD have focused on how to decrease the concentrations of Fe^{3+}, Al^{3+}, SO_4^{2-} and various toxic metals (Johnson and Hallberg, 2005). However, we propose that anthropogenic neutralization of AMD will also deplete Mo as Fe- and/or Al-based minerals form, as occurred at the ORR site. This process could disrupt the nitrogen cycle at the AMD site by decreasing nitrate removal and/or nitrogen fixation (Fig. 1) (Wu *et al*., 2006; Barron *et al*., 2009; Glass *et al*., 2012). In a previous study, the denitrification rate of sediment and surface water microcosms from AMD-impacted sediment decreased significantly when Fe^{3+}/Fe^{2+} was added, the pH values of which were between 3.17 and 4.52 (Baeseman *et al*., 2006). Based on the Mo depletion model proposed in our study, soluble MoO_4^{2-} in the

tested microcosms from the AMD-impacted environment would have been depleted by Fe precipitation that occurred when the pH increased, thus inhibiting nitrate reduction in the AMD-community. The lack of soluble and available Mo may decrease the rate of natural nitrate removal from contaminated groundwater via denitrification, particularly when appropriate electron donors are present. In addition to limiting nitrate reduction by a single organism as shown in this study, a lack of Mo may shift the microbial community structure such that other growth modes are more energetically favourable and become dominant, similar to what was found in estuarine environments (Howarth and Cole, 1985). It might be expected to take longer to re-establish nitrate to non-contaminant concentrations in these Mo-depleted environments (Colman *et al*., 2017).

The depletion of Mo in groundwater and freshwater environments could have additional environmental consequences. For example, Mo depletion in agricultural soils containing nitrate-based fertilizers could decrease denitrification rates compounding nitrate contamination issues (Glass *et al*., 2012). In addition, release of nitrate contaminated freshwater into the ocean results in eutrophication of nitrogen-limited estuarine and coastal ecosystems causing the spread of dead zones and hypoxia at affected river outlets (Smith *et al*., 1999; Diaz and Rosenberg, 2008). Moreover, limitation of nitrogen fixation by Mo availability could be relevant in areas without nitrate contamination. While environmental acid and metal contamination are clearly critical environmental concerns, it is important to also consider what nutrients are depleted as these contaminants are removed. The depletion of Mo in metal-rich acidic environments may be a key concern that needs to be considered in returning nitrate-contaminated environments to their natural state.

Experimental procedures

Molybdate depletion by iron or aluminium active precipitation

The synthetic groundwater composition was based on the previously published data (Smith *et al*., 2015) on the major inorganic ions measured in the highly contaminated well FW-126 (located 11.3 m down gradient from the S-3 ponds, see Supporting Information Table S1). Synthetic groundwater contained $Mg(NO_3)_2$ (8.9 mM), Na_2SO_4 (15.2 mM), $NaHCO_3$ (3 mM) and NaCl (10.5 mM). This data was based on the ion concentrations measured from contaminated groundwater (well FW-126; Supporting Information Table S1). It is important to note that Mo was not added to any of these solutions. The Mo that was present [up to ~ 50 nM in $Fe(NO_3)_3$ (20 mM)] originated as a contaminant in the various chemicals that we added to the solutions. Synthetic groundwater was acidified to pH 2.3, 3.8 or 2.6 by addition of trace metal grade $Fe(NO_3)_3$ (20 mM) (99.995% trace metal basis, MilliporeSigma, Missouri, USA), $Al(NO_3)_3$ (20 mM) (99.997% trace metal basis, MilliporeSigma) or a combination of $Fe(NO_3)_3$ (10 mM) and $Al(NO_3)_3$ (10 mM), respectively, to give a final concentration of 60 mM nitrate in each case. These acidifications were followed by precipitation of Fe or Al at pH 4.0, which was chosen to mimic the pH of the contaminated groundwater in well FW-126, or pH 6.7, which was used to simulate the neutralization of the contaminated groundwater by mixing with soils and neutral uncontaminated groundwater, induced by the addition of trace grade NaOH (99.99% TraceSELECT, Honeywell Fluka, Michigan, USA) and samples were allowed to settle for 30 min at room temperature. These procedures will be referred to as 'Fe treatment', 'Al treatment' or 'Fe + Al treatment'. Aliquots were taken prior to and after the pH adjustment, centrifuged (5000*g*, 20 min) and the concentrations of dissolved Fe, Al and Mo before and after Fe treatment, Al treatment and Fe + Al treatment were analyzed by inductively coupled plasma mass spectrometry (ICP-MS) to determine the effect of the treatment on Mo concentrations.

To investigate the effects of different anions on Mo depletion by Fe or Al precipitation, single anions Na_2SO_4 (15.2 mM), $NaHCO_3$ (3 mM), NaH_2PO_4 (5 mM) or NaCl (10.5 mM) or anion combinations of Na_2SO_4 (15.2 mM), $NaHCO_3$ (3 mM) and NaCl (10.5 mM) (SCC) were included exclusively in $Fe(NO_3)_3$ (20 mM) or $Al(NO_3)_3$ (20 mM) solutions with $Mg(NO_3)_2$ (8.9 mM), as Mg^{2+} is the major divalent cation in the ORR monitoring well FW-126 groundwater. Where indicated, molybdate was added as $(NH_4)_2MoO_4$ at final concentrations of 50 and 10 nM prior to the Fe or Al treatments, respectively, to provide a Mo concentration where changes could be easily measured. Then different solutions were adjusted to pH 6.7 to induce the precipitation of Fe and Al in 15 ml acid washed falcon tubes. Samples were incubated at room temperature for 30 min. Samples before the treatments and supernatants after treatments were collected for metal analysis by ICP-MS in order to determine the effect of anion interferences on Mo depletion at starting trace levels (pM to nM) of Mo concentration.

Molybdate adsorption to aluminium or iron precipitates

$Fe(NO_3)_3$ (20 mM), $Al(NO_3)_3$ (20 mM) or a 1:1 ratio thereof [10 mM $Fe(NO_3)_3$ and 10 mM $Al(NO_3)_3$] were added to synthetic groundwater solutions. The pHs of the mixtures were adjusted to either pH 4.0 or pH 6.7 by addition of NaOH (99.99% TraceSELECT). The solutions were then centrifuged at 5000*g* for 20 min to remove the

Fe and/or Al precipitates and 10 nM $(NH_4)_2MoO_4$ was added to the supernatant fractions and these were divided into two parts. One was mixed with the precipitate obtained from the prior centrifugation step and the other served as a control (with added Mo but with no precipitate). After equilibration for 16 h, the solutions were centrifuged at 5000*g* for 20 min, and the supernatants were analyzed by ICP-MS.

Growth of Pseudomonas fluorescens N2A2 in molybdate-depleted media

The standard growth medium contained 1.3 mM KCl, 2 mM $MgSO_4$, 0.1 mM $CaCl_2$, 0.3 mM NaCl, 30 mM $NaHCO_3$, 5 mM NaH_2PO_4 and 20 mM $NaNO_3$ with vitamins and minerals as described by Widdel and Bak (1992) except that molybdenum and tungsten were omitted. Glutamine (20 mM) was used as carbon source. Mo limited media were generated based on the standard medium and by using the Fe- or Al-treatments described above. Glutamine (20 mM), which is neutral, was used as carbon source instead of lactate to avoid interference with Mo depletion. Mo depleted medium solution which contained 1.3 mM KCl, 2 mM $MgSO_4$, 0.1 mM $CaCl_2$, 0.3 mM NaCl and 20 mM glutamine, 10 nM $(NH_4)_2MoO_4$ with vitamins and minerals was mixed with either $Fe(NO_3)_3$ (20 mM) or $Al(NO_3)_3$ (20 mM). The solutions were adjusted to pH 6.7 from pH 2.1 for Fe and pH 3.5 for Al to induce their precipitation. Then the supernatants were supplemented with $Fe(NO_3)_3$ (7.4 μM), Na_2SO_4 (2 mM), $NaHCO_3$ (30 mM) and NaH_2PO_4 (5 mM) which are required for N2A2 growth. $NaNO_3$ (60 mM) was used in untreated media to introduce nitrate. Untreated media, Fe/Al treated media and replete Fe/Al treated media with 10 nM MoO_4^{2-} added back in were inoculated with 1% (vol/vol) of *Pseudomonas fluorescens* N2A2 previously grown anaerobically in medium without added Mo on glutamine at 28°C. Samples were collected from pre-Fe/Al treatment solutions, post Fe/Al treatment solutions, post Fe/Al treatment solutions with N2A2 cells and post Fe/Al treatment solutions with N2A2 cells and replete Mo for ICP-MS metal analysis. Growth of N2A2 in untreated, Fe- or Al- treated, and Fe- or Al-treated and supplemented with 10 nM MoO_4^{2-} media were compared as indicated. Each growth was performed in triplicate and samples were collected every 5 h for the analyses described below.

Nitrate and nitrite measurements

Nitrate and nitrite were measured by the Griess colorimetric assay as previously described (Miranda *et al*., 2001). Samples were removed from growing cultures, centrifuged in a microcentrifuge to remove cells, and were assayed directly. Typically, 100 μl of diluted samples were mixed with 100 μl Griess reagents (MilliporeSigma) and incubated at 37°C for 1 h to determine the concentrations of nitrite produced during growth. To reduce the remaining nitrate to nitrite, 50 μl of diluted samples were mixed with 40 μl saturated VCl_3 (400 mg VCl_3 in 50 ml 1 M HCl). About 100 μl of the Griess reagent was added and the mixture was incubated at 37°C for 4 h before measuring absorption at 540 nm.

Nitrate reductase activity

Samples (5 ml) were removed from N2A2 cultures and cells were harvested by centrifugation (10 000*g* for 5 min). The pellet was re-suspended in 100 μl of water and lysed by sonication. The assay mixture (1.0 ml) consisted of 50 mM Tris/HCl buffer, pH 7.5, containing 0.5 mM methyl viologen and 1 mM potassium nitrate in an anaerobic sealed cuvette at 25°C. Sodium dithionite (4 mg/ml in 50 mM Tris–HCl buffer, pH 7.5) was added until an absorption at 578 nm of approximately 1.5. The reaction was initiated by the addition of the cell-free extract and nitrate reduction was monitored by the oxidation of reduced methyl viologen (Nason *et al*., 1971). One unit of total nitrate reductase activity catalyzed the reduction of 1 μmol of nitrate/min.

Metal analysis

Synthetic groundwater samples, processed sediment samples or culture samples were vortexed then diluted into 2% (vol/wt) trace-grade nitric acid (VWR, Pennsylvania, USA) in acid-washed polypropylene tubes and stored overnight at 4°C. Samples were analyzed using an Agilent 7900 ICP-MS fitted with MicroMist nebulizer, UHMI-spray chamber, Pt cones and an Octopole Reaction System (ORS) collision cell (Agilent Technologies, California, USA). The external calibration standards, IV-ICPMS-71A (Inorganic Ventures, Virginia, USA) and IV-ICPMS-71B (Inorganic Ventures, Virginia, USA), were used to create an 11-point curve from 0–500 (or 1000) ppb for each element and the internal calibration standard, IV-ICPMS-71D (Inorganic Ventures, Virginia, USA), was added to each sample. The data were collected as a 3-point peak pattern, 3 replicates, 100 sweeps/rep and various integration times (all > 0.3 s) with either no gas or He gas in the ORS collision cell. Data was processed using the nearest internal standard by mass and fitted to a linear curve though the calibration blank. Where indicated, environmental or biological replicates where averaged and reported with standard deviations (SD). The detection limits (DL) were calculated as three times the standard deviation of the calibration blank. All sediment

data are reported in mg/kg (i.e., ppm) and other data are reported in molar concentrations (i.e., mM–pM).

ORR sediment coring

The 800 cm vertical sediment core, EB-106, was located 21.1 m downstream from the southern corner of the S-3 pond, in an extremely contaminated region referred to as Area 3 (Moon *et al*., 2006; Li *et al*., 2018). The contaminated core (EB-106) is located 21.1 m from the edge of one of the ponds and 10.2 m from well FW-126. The sediment core spanned the vadose (0–300 cm), capillary fringe (300–350 cm) and saturated (350–800 cm) soil zones. The sediment was cored using a Geoprobe 6610 DT (Geoprobe, Salina, KS) dual tube hydraulic push continuous coring machine. The DT 350 that takes 8.9 cm diameter cores using PVC liners. The filled liners were cut in to approximately 22 cm segments at the field site and each end was immediately capped.

Metal extraction from ORR sediment core

The sediment core was cut into 23 cm sections, the end portion of each 22 cm segment was discarded, and an internal sample was manually homogenized. The moisture content and dry mass of three approximately 1 g samples of homogenized sediment were obtained by drying overnight in an oven at 102°C ± 2°C. Selected samples were then sequentially extracted for bioavailable metals by the BCR three-step sequential extraction procedure (Rauret, 1998), where the soil was sequentially extracted with a weakly acidic (0.11 M acetic acid) solution, a reducing agent (0.5 M hydroxylammonium chloride) and an oxidizing agent (8.8 M hydrogen peroxide at 85°C). The first step involves extraction of the sediment with a weak acid (0.11 M acetic acid), which removes any porewater metals as well as metals that are precipitated with carbonate and are easily solubilized (Kazi *et al*., 2005). The second step is the subsequent reductive extraction by incubation with 0.5 M hydroxylammonium chloride, which will release metals bound to metal oxides (Kazi *et al*., 2005). The third step is oxidative extraction and involves digesting the sediment remaining from the reductive extraction using 8.8 M H_2O_2 at 85°C. This extraction also releases metals from organic matter, such as high molecular weight humic compounds (Kazi *et al*., 2005). Supernatants from the three extraction steps were diluted 1:40 in 2% (vol/vol) nitric acid for ICP-MS analysis. An additional 1 g of soil (dry weight) from each segment was microwave digested in 10 ml of concentrated nitric acid as described in EPA protocol 3051A (Link *et al*., 1998) to determine the total metal content of sediment. After microwave digestion, samples were diluted to 100 ml total volume with ddH_2O. For ICP-MS analysis, a 1 ml portion was diluted with 4 ml of ddH_2O resulting in 2% (vol/vol) nitric acid in the samples. These samples were further diluted 1:5 and 1:50 in 2% (vol/vol) nitric acid before being analyzed by ICP-MS.

Acknowledgements

The authors wish to thank Kenneth Lowe and Dominique Joyner for their invaluable help in collecting sediment samples. This material by ENIGMA (Ecosystems and Networks Integrated with Genes and Molecular Assemblies) (http://enigma.lbl.gov), a Scientific Focus Area Program at Lawrence Berkeley National Laboratory, is based upon work supported by the U.S. Department of Energy, Office of Science, Office of Biological and Environmental Research, under contract number DE-AC02-05CH11231.

References

Allada, R. K., Navrotsky, A., Berbeco, H. T., and Casey, W. H. (2002) Thermochemistry and aqueous solubilities of hydrotalcite-like solids. *Science* **296**: 721–723.

Baeseman, J., Smith, R., and Silverstein, J. (2006) Denitrification potential in stream sediments impacted by acid mine drainage: effects of pH, various electron donors, and iron. *Microb Ecol* **51**: 232–241.

Barron, A. R., Wurzburger, N., Bellenger, J. P., Wright, S. J., Kraepiel, A. M., and Hedin, L. O. (2009) Molybdenum limitation of asymbiotic nitrogen fixation in tropical forest soils. *Nat Geosci* **2**: 42–45.

Beck, M., Dellwig, O., Schnetger, B., and Brumsack, H.-J. (2008) Cycling of trace metals (Mn, Fe, Mo, U, V, Cr) in deep pore waters of intertidal flat sediments. *Geochim Cosmochim Acta* **72**: 2822–2840.

Bouchard, D. C., Williams, M. K., and Surampalli, R. Y. (1992) Nitrate contamination of groundwater: sources and potential health effects. *J Am Water Works Assoc* **84**: 85–90.

Brooks, S.C. (2001) *Waste Characteristics of the Former S-3 Ponds and Outline of Uranium Chemistry Relevant to NABIR Field Research Center studies.* Oak Ridge, TN: ORNL Oak Ridge National Laboratory (US).

Cao, G.-H., Yan, S.-M., Yuan, Z.-K., Wu, L., and Liu, Y.-F. (1998) A study of the relationship between trace element Mo and gastric cancer. *World J Gastroenterol* **4**: 55–56.

Colman, D. R., Poudel, S., Stamps, B. W., Boyd, E. S., and Spear, J. R. (2017) The deep, hot biosphere: twenty-five years of retrospection. *Proc Natl Acad Sci USA* **114**: 6895–6903.

Cronan, C. S., and Schofield, C. L. (1979) Aluminum leaching response to acid precipitation: effects on high-elevation watersheds in the northeast. *Science* **204**: 304–306.

Diaz, R. J., and Rosenberg, R. (2008) Spreading dead zones and consequences for marine ecosystems. *Science* **321**: 926–929.

Gorchev, H. G., and Ozolins, G. (1984) WHO guidelines for drinking-water quality. *WHO Chron* **38**: 104–108.

Giles, M., Morley, N., Baggs, E. M., and Daniell, T. J. (2012) Soil nitrate reducing processes drivers, mechanisms for

spatial variation, and significance for nitrous oxide production. *Front Microbiol* **3**: 407.

Glass, J. B., Axler, R. P., Chandra, S., and Goldman, C. R. (2012) Molybdenum limitation of microbial nitrogen assimilation in aquatic ecosystems and pure cultures. *Front Microbiol* **3**: 331.

Goldberg, S. (2010) Competitive adsorption of molybdenum in the presence of phosphorus or sulfur on gibbsite. *Soil Sci* **175**: 105–110.

Gruber, N., and Galloway, J. N. (2008) An earth-system perspective of the global nitrogen cycle. *Nature* **451**: 293–296.

Gustafsson, J. P. (2003) Modelling molybdate and tungstate adsorption to ferrihydrite. *Chem Geol* **200**: 105–115.

Härtig, E., Schiek, U., Vollack, K.-U., and Zumft, W. G. (1999) Nitrate and nitrite control of respiratory nitrate reduction in denitrifying *Pseudomonas stutzeri* by a two-component regulatory system homologous to NarXL of *Escherichia coli*. *J Bacteriol* **181**: 3658–3665.

Helz, G. R., Miller, C. V., Charnock, J. M., Mosselmans, J. F. W., Pattrick, R. A. D., Garner, C. D., and Vaughan, D. J. (1996) Mechanism of molybdenum removal from the sea and its concentration in black shales: EXAFS evidence. *Geochim Cosmochim Acta* **60**: 3631–3642.

Hemme, C. L., Deng, Y., Gentry, T. J., Fields, M. W., Wu, L., Barua, S., *et al*. (2010) Metagenomic insights into evolution of a heavy metal-contaminated groundwater microbial community. *ISME J* **4**: 660–672.

Howarth, R. W., and Cole, J. J. (1985) Molybdenum availability, nitrogen limitation, and phytoplankton growth in natural waters. *Science* **229**: 653–655.

Hug, L. A., Thomas, B. C., Sharon, I., Brown, C. T., Sharma, R., Hettich, R. L., *et al*. (2016) Critical biogeochemical functions in the subsurface are associated with bacteria from new phyla and little studied lineages. *Environ Microbiol* **18**: 159–173.

Istok, J., Senko, J., Krumholz, L. R., Watson, D., Bogle, M. A., Peacock, A., *et al*. (2004) In situ bioreduction of technetium and uranium in a nitrate-contaminated aquifer. *Environ Sci Technol* **38**: 468–475.

Jackson, M. L., Zhang, J. Z., Li, C. S., and Martin, D. F. (1986) The geochemical availability of soil Zn and Mo in relation to stomach and esophageal cancer in the People's Republic of China and U.S.a. *Appl Geochem* **1**: 487–492.

Johnson, D. B., and Hallberg, K. B. (2005) Acid mine drainage remediation options: a review. *Sci Total Environ* **338**: 3–14.

Jones, S. (1998) *Evaluation of Calendar Year 1997 Groundwater and Surface Water Quality Data for the Upper East Fork Poplar Creek Hydrogeologic Regime at the US Department of Energy Y-12 Plant, Oak Ridge, Tennessee.* Oak Ridge, TN: Oak Ridge Y-12 Plant.

Kazi, T., Jamali, M., Kazi, G., Arain, M., Afridi, H., and Siddiqui, A. (2005) Evaluating the mobility of toxic metals in untreated industrial wastewater sludge using a BCR sequential extraction procedure and a leaching test. *Anal Bioanal Chem* **383**: 297–304.

Khanna, S., Udas, A. C., Kumar, G. K., Suvarna, S., and Karjodkar, F. R. (2013) Trace elements (copper, zinc, selenium and molybdenum) as markers in oral sub mucous fibrosis and oral squamous cell carcinoma. *J Trace Elem Med Biol* **27**: 307–311.

Klotz, M. G., and Stein, L. Y. (2008) Nitrifier genomics and evolution of the nitrogen cycle. *FEMS Microbiol Lett* **278**: 146–156.

Kornegay, F., West, D., McMahon, L., Murphy, J., Shipe, L., and Koncinski, W. (1994) *Oak ridge reservation annual site environmental report for 1993.* In: ES/ESH-47, Martin Marietta Energy Systems, Inc.

Li, B., Wu, W. M., Watson, D. B., Cardenas, E., Chao, Y. Q., Phillips, D. H., *et al*. (2018) Bacterial community shift and coexisting/coexcluding patterns revealed by network analysis in a uranium-contaminated site after bioreduction followed by reoxidation. *Appl Environ Microbiol* **84**: AEM-02885.

Link, D. D., Walter, P. J., and Kingston, H. (1998) Development and validation of the new EPA microwave-assisted leach method 3051A. *Environ Sci Technol* **32**: 3628–3632.

Miranda, K. M., Espey, M. G., and Wink, D. A. (2001) A rapid, simple spectrophotometric method for simultaneous detection of nitrate and nitrite. *Nitric Oxide* **5**: 62–71.

Moon, J. W., Roh, Y., Phelps, T. J., Phillips, D. H., Watson, D. B., Kim, Y. J., and Brooks, S. C. (2006) Physicochemical and mineralogical characterization of soil-saprolite cores from a field research site, Tennessee. *J Environ Qual* **35**: 1731–1741.

Morford, J. L., Martin, W. R., Kalnejais, L. H., François, R., Bothner, M., and Karle, I.-M. (2007) Insights on geochemical cycling of U, re and Mo from seasonal sampling in Boston Harbor, Massachusetts, USA. *Geochim Cosmochim Acta* **71**: 895–917.

Moura, J. J. G., Brondino, C. D., Trincao, J., and Romao, M. J. (2004) Mo and W bis-MGD enzymes: nitrate reductases and formate dehydrogenases. *J Biol Inorg Chem* **9**: 791–799.

Nason, A., Lee, K.-Y., Pan, S.-S., Ketchum, P. A., Lamberti, A., and DeVries, J. (1971) *In vitro* formation of assimilatory reduced nicotinamide adenine dinucleotide phosphate: nitrate reductase from a Neurospora mutant and a component of molybdenum-enzymes. *Proc Natl Acad Sci USA* **68**: 3242–3246.

Nolan, B. T., and Hitt, K. J. (2006) Vulnerability of shallow groundwater and drinking-water wells to nitrate in the United States. *Environ Sci Technol* **40**: 7834–7840.

Nolan, B. T., Ruddy, B. C., Hitt, K. J., and Helsel, D. R. (1998) A national look at nitrate contamination of ground water. *Water Cond Purification* **39**: 76–79.

Nordstrom, D. K. (2015) Baseline and premining geochemical characterization of mined sites. *Appl Geochem* **57**: 17–34.

Nouri, M., Chalian, H., Bahman, A., Mollahajian, H., Ahmadi-Faghih, M., Fakheri, H., and Soroush, A. (2008) Nail molybdenum and zinc contents in populations with low and moderate incidence of esophageal cancer. *Arch Iran Med* **11**: 392–396.

Paikaray, S., and Hendry, M. J. (2013) In situ incorporation of arsenic, molybdenum, and selenium during precipitation of hydrotalcite-like layered double hydroxides. *Appl Clay Sci* **77**: 33–39.

Palmer, K., Drake, H. L., and Horn, M. A. (2010) Association of novel and highly diverse acid-tolerant denitrifiers with

N_2O fluxes of an acidic fen. *Appl Environ Microbiol* **76**: 1125–1134.

Palmer, K., Biasi, C., and Horn, M. A. (2012) Contrasting denitrifier communities relate to contrasting N_2O emission patterns from acidic peat soils in arctic tundra. *ISME J* **6**: 1058–1077.

Powlson, D. S., Addiscott, T. M., Benjamin, N., Cassman, K. G., de Kok, T. M., van Grinsven, H., *et al*. (2008) When does nitrate become a risk for humans? *J Environ Qual* **37**: 291–295.

Qu, Z., Bakken, L. R., Molstad, L., Frostegård, Å., and Bergaust, L. L. (2016) Transcriptional and metabolic regulation of denitrification in P aracoccus denitrificans allows low but significant activity of nitrous oxide reductase under oxic conditions. *Environ Microbiol* **18**: 2951–2963.

Rauret, G. (1998) Extraction procedures for the determination of heavy metals in contaminated soil and sediment. *Talanta* **46**: 449–455.

Revil, A., Skold, M., Karaoulis, M., Schmutz, M., Hubbard, S. S., Mehlhorn, T. L., and Watson, D. B. (2013) Hydrogeophysical investigations of the former S-3 ponds contaminant plumes, oak ridge integrated field research challenge site, Tennessee. *Geophysics* **78**: EN29–EN41.

Salmimies, R. (2012) Acidic dissolution of iron oxides and regeneration of a ceramic filter medium. *Acta Univ Lappeenrantaensis* **6**: 143–156.

Salmimies, R., Mannila, M., Juha, J., and Häkkinen, A. (2011) Acidic dissolution of magnetite: experimental study on the effects of acid concentration and temperature. *Clays Clay Miner* **59**: 136–146.

Sánchez-España, J., Yusta, I., Gray, J., and Burgos, W. D. (2016) Geochemistry of dissolved aluminum at low pH: extent and significance of Al–Fe (III) coprecipitation below pH 4.0. *Geochim Cosmochim Acta* **175**: 128–149.

Schwarz, G., Mendel, R. R., and Ribbe, M. W. (2009) Molybdenum cofactors, enzymes and pathways. *Nature* **460**: 839–847.

Showe, M. K., and DeMoss, J. (1968) Localization and regulation of synthesis of nitrate reductase in *Escherichia coli*. *J Bacteriol* **95**: 1305–1313.

Smedley, P. L., and Edmunds, W. M. (2002) Redox patterns and trace-element behavior in the east midlands triassic sandstone aquifer, UK. *Groundwater* **40**: 44–58.

Smedley, P. L., and Kinniburgh, D. G. (2017) Molybdenum in natural waters: a review of occurrence, distributions and controls. *Appl Geochem* **84**: 387–432.

Smith, H. D., Parkinson, G. M., and Hart, R. D. (2005) In situ absorption of molybdate and vanadate during precipitation of hydrotalcite from sodium aluminate solutions. *J Cryst Growth* **275**: e1665–e1671.

Smith, M. B., Rocha, A. M., Smillie, C. S., Olesen, S. W., Paradis, C., Wu, L., *et al*. (2015) Natural bacterial communities serve as quantitative geochemical biosensors. *MBio* **6**: e00326–e00315.

Smith, V. H., Tilman, G. D., and Nekola, J. C. (1999) Eutrophication: impacts of excess nutrient inputs on freshwater, marine, and terrestrial ecosystems. *Environ Pollut* **100**: 179–196.

Thorgersen, M. P., Lancaster, W. A., Vaccaro, B. J., Poole, F. L., Rocha, A. M., Mehlhorn, T., *et al*. (2015) Molybdenum availability is key to nitrate removal in contaminated groundwater environments. *Appl Environ Microbiol* **81**: 4976–4983.

Vergnes, A., Gouffi-Belhabich, K., Blasco, F., Giordano, G., and Magalon, A. (2004) Involvement of the molybdenum cofactor biosynthetic machinery in the maturation of the *Escherichia coli* nitrate reductase a. *J Biol Chem* **279**: 41398–41403.

Watanabe, T., Motoyama, H., and Kuroda, M. (2001) Denitrification and neutralization treatment by direct feeding of an acidic wastewater containing copper ion and high-strength nitrate to a bio-electrochemical reactor process. *Water Res* **35**: 4102–4110.

Watson, D., Kostka, J., Fields, M., and Jardine, P. (2004) *The Oak Ridge Field Research Center Conceptual Model*. Oak Ridge, TN: NABIR Field Research Center.

Wichard, T., Mishra, B., Kraepiel, A., and Myneni, S. (2008) Molybdenum speciation and bioavailability in soils. *Geochim Cosmochim Acta* **72**: A1019.

Widdel, F., and Bak, F. (1992)Gram-negative mesophilic sulfate-reducing bacteria . In *The Prokaryotes*, Balows, A., Trüper, H., Dworkin, M., Harder, W., and Schleifer, K.-H. (eds). New York, NY: Springer, pp. 3352–3378.

Wu, W.-M., Carley, J., Fienen, M., Mehlhorn, T., Lowe, K., Nyman, J., *et al*. (2006) Pilot-scale in situ bioremediation of uranium in a highly contaminated aquifer. 1. Conditioning of a treatment zone. *Environ Sci Technol* **40**: 3978–3985.

Zhang, Y., and Gladyshev, V. N. (2008) Molybdoproteomes and evolution of molybdenum utilization. *J Mol Biol* **379**: 881–899.

Zumft, W. G. (1997) Cell biology and molecular basis of denitrification. *Microbiol Mol Biol Rev* **61**: 533–616.

Supporting Information

Additional Supporting Information may be found in the online version of this article at the publisher's web-site:

Appendix S1: Supporting Information